Two Distinct Carpal Bone Motion Patterns Revealed from a Kinematic Model

Bardiya Akhbari[1], Douglas C. Moore[2], David H. Laidlaw[1], Edward Akelman[2], Arnold-Peter C. Weiss[2], Scott W. Wolfe[3], Joseph J. Crisco[1, 2]
[1]Brown University, Providence, RI, [2]Rhode Island Hospital, Providence, RI, [3]Hospital for Special Surgery, New York, NY
bardiya_akhbari@brown.edu

Disclosures: B. Akhbari: None. D. Moore: None. D. Laidlaw: None. E. Akelman: [1, 7A]. A-P Weiss: None. S. Wolfe: [1,2,3B,5,7B,8]. J. Crisco: [3B,7A,8].

INTRODUCTION: Understanding carpal joint kinematics is essential for understanding the normal joint function and advancing the treatment of wrist pathologies. The wrist is generally considered a two degrees-of-freedom (DOF) joint with all motions reflecting the combination of flexion-extension (FE) and radial-ulnar deviation (RU), accomplished by kinematic reduction of the 42 DOFs of the individual carpal bones. While previous studies have demonstrated how individual bones move relative to one another (e.g., minimal motion of scaphoid relative to lunate in dart-thrower's path[1]), or how groups of carpal bones appear to function as units (e.g., small relative motion between hamate, capitate, and trapezoid[2]), a unified model of carpal kinematics across all wrist motions is lacking. To address this, we assembled a large database of *in-vivo* wrist motions from several of our previous CT image-based kinematic studies[3-5], and developed a mathematical model of the carpal kinematics as a function of wrist position. In this paper, we present analyses of the motion patterns of the distal (hamate, capitate, trapezoid, and trapezium) and proximal (triquetrum, lunate, and scaphoid) rows of carpal bones.

METHODS: The database was assembled from eleven previous studies on carpal bone postures that included 1063 wrist positions of 88 healthy individuals (Figure 1). Kinematics of the carpal bones were calculated from the neutral wrist positions to each of the corresponding study positions using established methodologies and an overall approach similar to our previous description of an *in-vivo* carpal bone database[1]. Kinematic transformations were described using the helical axis of motion parameters, and reported in a radius-based anatomic coordinate system[6]. Rotations were decomposed into FE, RU deviation, and Supination-Pronation (SP) components. Translations were the displacement of the origin of the carpal bone inertial coordinate system ((Distal-Proximal Translation (DPT), Radial-Ulnar Translation (RUT), and Volar-Dorsal Translation (VDT)), and were scaled by the cube root of capitate volume, to eliminate the influence of bone size[7]. We used the capitate position (FE and RU) as the measure of wrist position[8]. A quadratic polynomial as a function of wrist FE and RU ($WRIST_{FE}$ and $WRIST_{RU}$) was used to mathematically model the forty-two-individual bone DOFs ($BONE_{DOF}$) using a least-squares optimization method with a leave-one-out cross-validation strategy. 932 motions were randomly selected to train the model (78 subjects, 101 wrists), and 131 motions (10 subjects, 15 wrists) were reserved for testing the model (*Test Set*). The model with the lowest root-mean-squared-error (RMSE) in the cross-validation procedure was then evaluated by calculating the R^2 and RMSE using the *Test Set* data. A "zero-motion" path (ZM) was defined for each bone and each DOF as the path of wrist motion associated with minimal rotation (<0.01°) or translation (<0.01mm) of that DOF for that bone. Linear regression ($p < 0.05$) was used to calculate the lower and upper confidence intervals (LCI and UCI; Table 1) of the ZM slope (on a plot of wrist position, i.e., Figure 2) of each bone and DOF.

RESULTS: The mathematical model performed well on the *Test Set* in predicting FE ($R^2 > 0.92$, and RMSE < 5.8°) for all carpal bones. The model performed less well (i.e., higher RMSE) in predicting RU deviation ($R^2 > 0.6$, and RMSE < 9°), VDT ($R^2 > 0.65$, and RMSE < 3 mm), and it performed poorest for RUT, DPT ($R^2 < 0.6$, and RMSE < 4 mm), and SP ($R^2 < 0.5$, and RMSE < 8°). The ZM plots describing minimal carpal bone FE and VDT (Figure 2) are depicted as representative. The ZM slopes for carpal bone FE and VDT were different for all carpal bones ($p < 0.01$) (Table 1). The slopes were between -0.1 to 0.1 for hamate, triquetrum, and lunate (distal row), while they were between 0.6 to 1.2 for triquetrum, lunate, and scaphoid (proximal row) (Table 1). The same comparison for VDT showed -0.3 to 0.3 slope range for the distal row, and 1.1 to 1.7 slope range for the proximal row.

DISCUSSION: The purpose of this study was to develop a mathematical model to explore patterns in carpal bone motion using a large database of carpal bone kinematics. We generated a quadratic mathematical model that it had the lowest RMSE and highest R^2 on the test set for FE, RU, and VDT DOFs, and they were moderate on RUT, DPT and SP. The model revealed patterns of motion that were similar among bones in the distal row and among bones in the proximal row. The distal row was tightly entrained to the capitate's motion, while the bones in the proximal row moved more independently. Encouragingly, our results on FE and VDT are generally consistent with the literature[1], with FE and VDT of the distal row minimized during radioulnar deviation, while similar motions of the bones in the proximal row were minimized along the path from wrist radial extension to ulnar flexion (dart thrower's motion). The proposed model is a first step toward locating the carpal bones at any unique wrist position, and our hope is that the free distribution of this dataset will facilitate the development of an accurate model that reliably predicts the carpal bone kinematics.

SIGNIFICANCE: The mathematical model constructed from this study will be helpful for clinical thinking and animating the wrist motion. Also, we showed that the distal row of carpal bones (i.e., hamate, capitate, trapezoid, and trapezium) move together, along the anatomical axis of wrist motion, while the bones in the proximal row (i.e., triquetrum, lunate, and scaphoid) move in a path oblique to that axis.

ACKNOWLEDGEMENTS: This work is funded by NIH R01-AR44005, HD052127, and AR053648.

REFERENCES: [1] Crisco. *J Bone Joint Surg* **2005**. [2] Taleisnik. *J Hand Surg 1976.* [3] D.C. Moore, *J Bio* **2007**. [4] Crisco, *J Bio Eng* **2015**. [3] Kamal, *J Bone Joint Surg Am* **2012**. [5] Leventhal, *J Hand Surg Am* **2010**. [6] Wu, *J Bio* **2005**. [7] M.J. Rainbow, *J Biomech Eng* **2008**. [8] C.P. Neu, *J Biomech* **2001**.

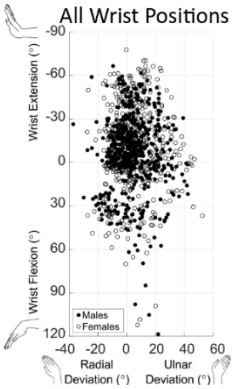

Figure 1. The wrist positions, as defined by the orientation of the capitate, for all subjects included in the database. Every point reflects the wrist position for a specific task: the neutral pose is at the origin (0,0).

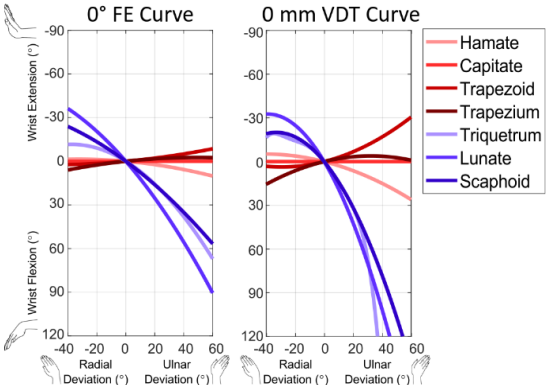

Figure 2. Zero-motion path (ZM) of a degree-of-freedom (DOF) for a carpal bone shows the path of the wrist motion when that carpal bone has a minimal displacement/rotation in that DOF. For example, a ZM for flexion-extension of capitate bone must be a curve passing through the whole radial-ulnar deviation range while flexion-extension angle is 0° (because we define the wrist motion as the motion of the capitate bone).

FE Zero Motion Slope's CI

BONE	LCI	UCI
Hamate	0.09	0.11
Trapezoid	-0.09	-0.08
Trapezium	-0.1	-0.09
Triquetrum	0.6	0.7
Lunate	1.1	1.2
Scaphoid	0.7	0.8

VDT Zero Motion Slope's CI

BONE	LCI	UCI
Hamate	0.2	0.3
Trapezoid	-0.3	-0.2
Trapezium	-0.3	-0.2
Triquetrum	1.1	1.3
Lunate	1.5	1.7
Scaphoid	1.1	1.3

Table 1. The lower and upper confidence interval (CI) of ZM slopes for FE and VDT revealed distinct patterns for the proximal row (slopes < 0.3), and the distal row (slopes > 0.6) of carpal bones.